THE ROYAL SOCIETY

doi 10.1098/rspb.2001.1666

Lift generation by the avian tail

W. J. Maybury[1]†, J. M. V. Rayner[2*] and L. B. Couldrick[2]

[1]*School of Biological Sciences, University of Bristol, Woodland Road, Bristol BS8 1UG, UK*
[2]*School of Biology, University of Leeds, Clarendon Way, Leeds LS2 9JT, UK*

Variation with tail spread of the lift generated by a bird tail was measured on mounted, frozen European starlings (*Sturnus vulgaris*) in a wind tunnel at a typical air speed and body and tail angle of attack in order to test predictions of existing aerodynamic theories modelling tail lift. Measured lift at all but the lowest tail spread angles was significantly lower than the predictions of slender wing, leading edge vortex and lifting line models of lift production. Instead, the tail lift coefficient based on tail area was independent of tail spread, tail aspect ratio and maximum tail span. Theoretical models do not predict bird tail lift reliably and, when applied to tail morphology, may underestimate the aerodynamic optimum tail feather length. Flow visualization experiments reveal that an isolated tail generates leading edge vortices as expected for a low-aspect ratio delta wing, but that in the intact bird body–tail interactions are critical in determining tail aerodynamics: lifting vortices shed from the body interact with the tail and degrade tail lift compared with that of an isolated tail.

Keywords: bird; flight; tail; lift; aerodynamics; body–tail interaction

1. INTRODUCTION

The aerodynamic functions of the avian tail are complex and versatile, serving to aid manoeuvrability, improve stability, control pitching movements, enhance lift generation at low flight speeds and reduce body drag at cruising flight speeds (Pennycuick 1975; Norberg 1990; Thomas 1993, 1996; Maybury & Rayner 2001). It has also been proposed that, in some species at least, the tail plays a communication role in mating behaviour and display. Whether sexual selective pressures outweigh natural selection for aerodynamic performance in determining tail morphology has been widely and hotly debated (e.g. Evans & Thomas 1997; Møller *et al.* 1998; Barbosa & Møller 1999; Buchanan & Evans 2000). This debate about tail function has concentrated on species with large and ornamented tails (in particular the barn swallow *Hirundo rustica*) (e.g. Møller 1994; Møller *et al.* 1995, 1998; Barbosa & Møller 1999; Buchanan & Evans 2000) and has tended to obscure the fact that remarkably little is known about tail aerodynamics in bird species with more typical tails without ornaments or relatively long rectrices.

Theoretical predictions of tail lift (e.g. Thomas 1993) have been based on the slender wing model (Jones 1946), but neither this nor alternative aerodynamic models that are potentially applicable to bird tails have hitherto been tested experimentally. Here we report on measurements of tail lift in the European starling *Sturnus vulgaris*. The morphology of the starling tail is typical of passeriform birds, with an approximately rectangular planform when furled; unlike the barn swallow tail, it has not been implicated in sexual selection and the outermost rectrices are not thought to control posture by self-cambering (Norberg 1994). We also report the first visualizations of the air flow around the tail and use these results to test aerodynamic models of tail lift and discuss aerodynamic interactions between the tail and the body.

*Author for correspondence (j.m.v.rayner@leeds.ac.uk).
†Present address: Westland Helicopters Limited, Box 231, Lysander Road, Yeovil, Somerset BA20 2YB, UK.

2. MATERIAL AND METHODS

(a) *Experimental design*

Measurements of lift were conducted on a mounted specimen of European starling (*S. vulgaris*); flow visualization observations were made on mounted starlings and on model and mounted starling tails. We used an open circuit Eiffel-pattern wind tunnel (Maybury 2000) with a closed working section of $0.52\,\mathrm{m} \times 0.52\,\mathrm{m} \times 1.00\,\mathrm{m}$ in dimension at air speeds of $4.9\,\mathrm{m\,s^{-1}}$ (at this speed the RMS turbulence in the centre of the working section around the bird was less than 0.35%); this speed is below the normal cruising flight speeds of starlings, but is in the speed range where the tail may be expected to be used to enhance lift in acceleration and deceleration. In starlings the tail is deployed in sustained undulating flight at this mean air speed (Rayner *et al.* 2001).

Birds were frozen with minimal disturbance to their feather alignment; their wings were removed at the shoulder and their feet and legs at the knee joint, leaving a smooth feathered body profile. Body feathers were treated with a light, even coating of hair wax (Pennycuick *et al.* 1988) so that feathers retained their position but some compliance remained in the integument; wires concealed under the feathers maintained posture. Tail posture was maintained by bonding each end of a 0.9-mm steel rod to the tips of the outer rectrices using cyanoacrylate adhesive (Loctite Super Glue®, Loctite UK Limited, Welwyn Garden City, Herts, UK), with the middle of the rod concealed under the covert feathers. Body and tail posture were determined from observation of video films of starlings flying in a wind tunnel, which were made in the course of a different study (Ward *et al.* 1999; Rayner *et al.* 2001). The tail was spread by symmetrically moving the outer rectrices to the desired position; the middle rectrices passively adopted a natural formation, with the tail having an approximately triangular planform with a slightly concave or straight trailing edge. The angle of spread θ (from 0 to 32°) was defined as half the angle between two straight lines projected along the outer rectrices. The maximum

Received 20 December 2000 *Accepted* 13 March 2001

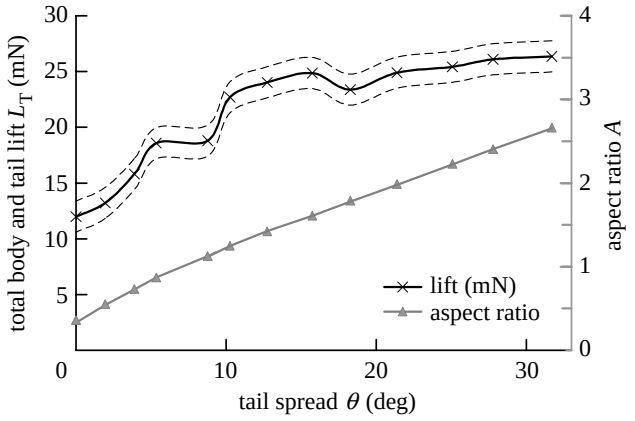

Figure 1. Measured total body and tail lift L_T against tail spread θ (half of apex angle). The dashed lines show a standard deviation measurement error of ± 1.39 mN from balance calibration. For details of the methods see the text. The figure also shows the near-linear relationship between tail spread θ and the aspect ratio A.

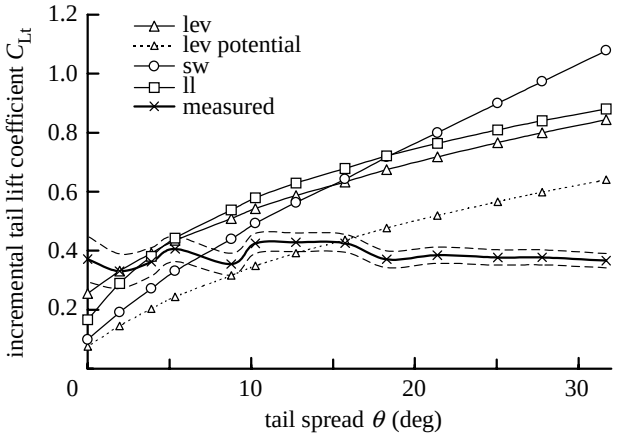

Figure 2. Measured incremental tail lift coefficient C_{Lt} (equation (2)) against the angle of tail spread θ for a starling body and tail with the tail set at $\alpha = 15^\circ$ at air speed $V = 4.9\ \mathrm{m\,s^{-1}}$. The dashed lines show the standard deviation error of C_{Lt}. For comparison, the incremental lift coefficients predicted by the slender wing, leading edge vortex and lifting line models are also shown (see § 3 for formulae), together with the potential component of the leading edge vortex model. For isolated triangular wings, the slender wing model is realistic only for low aspect ratio wings ($A < 1$ and $\theta < 11^\circ$) at low α ($< 5^\circ$), the leading edge vortex model is a good approximation for $A < 4$ and $\theta < 45^\circ$ (Hoerner 1975) and the lifting line models is expected to be more realistic at higher A and θ.

tail span b_{max} and planform area S_t of the tail, including its covert feathers, were measured for each angle of spread.

(b) *Lift measurements*

Birds were mounted on a sting passing laterally through the body close to the shoulder joint and the centre of mass of the body. Lift L (and also drag) (see Maybury & Rayner 2001) was measured from the deflection of strain gauges mounted on the sting (design following Bonser & Rayner 1996). The output of the strain gauge bridge was collected through a commercial strain gauge amplifier (RS Components Ltd, Corby, Northants, UK) and digitized by a PC-based analogue to digital converter (DAS 50, Keithley Instruments Inc., Cleveland, OH, USA) at a sampling rate of 300 Hz for 8190 readings per channel and subsequently filtered and averaged. Force measurements were highly repeatable in these and other similar experiments and the standard deviation (s.d.) error from calibration experiments was ± 1.39 mN. Because the body of a starling is small relative to the wind tunnel cross-section, blockage corrections (Rae & Pope 1984) applied to the air speed and lift were small (0.7–0.8%) and were neglected.

Lift is expressed in terms of lift coefficients, which are defined as

$$C_L = L/0.5\rho S_t V^2, \quad (1)$$

where V is the air speed and S_t is the tail planform area. Air density ρ was taken as $1.225\ \mathrm{kg\,m^{-3}}$ and dynamic viscosity μ (in definition of Reynolds number Re based on frontal projected body diameter) as $1.82 \times 10^{-5}\ \mathrm{kg\,m^{-1}s^{-1}}$.

The effect of tail posture on tail lift L_t was determined by measuring the total body and tail lift L_T at air speed $V = 4.9\ \mathrm{m\,s^{-1}}$ with body angle of attack $\alpha_b = 5^\circ$ (as observed in starlings at this speed), with tail angle of attack α relative to the free stream of 15° at 13 increasing tail spread angles from 0 to 32° (aspect ratio 0.36–2.66) (figure 1). Body lift L_b was defined here and measured as the lift at the same α_b and air speed with the tail furled ($\theta = 0$) and held parallel to the body (and, thus, at $\alpha = 5^\circ$). The effect of varying tail spread is measured through the incremental tail lift coefficient C_{Lt}, which is defined as

$$C_{LT}(\alpha = 15^\circ, \theta) = [L_T(\alpha = 15^\circ, \theta) - L_b(\alpha = 5^\circ, \theta = 0^\circ)]/0.5\rho S_t V^2. \quad (2)$$

Statistical procedures and other data manipulations were undertaken in MS Excel 97.

3. AERODYNAMIC THEORY

(a) *Theoretical predictions*

A number of theoretical models are available for predicting the lift from an avian tail. We follow Thomas (1993) in modelling the tail as a delta wing, that is as a thin, flat, triangular, slender wing with a straight, trailing edge, with the same area S_t, tail spread b and angle of spread θ as measured. For a triangular tail, the aspect ratio $A = 4\tan\theta$. Slender wing and delta wing theories are likely to be most appropriate for predicting lift from a surface of this kind; we also include the lifting line model for a high-aspect ratio wing. The downstream wake of an isolated lifting surface must incorporate trailing vortices that convect momentum downwards; the models differ in the origin of the wake vortices. Slender wing models implicitly assume that trailing vortices are shed at the widest points of the wing and in leading edge vortex models the vortices are shed from the swept leading edge of the wing, while in lifting line models they are shed from the trailing edge. Full derivations of the models are given in the aeronautical literature. Here we quote formulae for predicting lift and evaluate them in figure 2.

(b) *Slender wing model*

The slender wing model (sw) (Jones 1946) is a linearized theory that is appropriate to a thin and flat wing at

low α. The meaning of 'slender' is that the wing- or tail span increases slowly with streamwise position behind the wing apex. For triangular wings the model is restricted to a low aspect ratio, below *ca.* 1 and to α below *ca.* 5° (Hoerner 1975). Lift L_{sw} can be predicted by modelling the potential flow around a wing section (Jones 1946, 1990; Thomas 1993) or by linearized lifting surface methods (Jones 1990; Katz & Plotkin 1991). Lift

$$L_{sw} = \pi\rho V^2 b_{max}^2 \alpha/4, \tag{3}$$

is determined only by the air speed V, angle of attack α and maximum continuous tail span b_{max}. Subject to the low aspect ratio and low α assumptions the slender wing model should be applicable to all tail shapes, but should the tail taper only that portion upstream of the largest continuous span contributes to lift. It is counter-intuitive that lift is independent of tail length, particularly for straight or graduated tails. Since the aspect ratio $A = b_{max}^2/S_t$, the lift coefficient can be written

$$C_{L,sw} = \pi A\alpha/2. \tag{4}$$

(c) *Leading edge vortex model*

The slender wing model is severely restricted by its assumptions of a low α and of a gradual increase in wingspan from tip to trailing edge. It has frequently been demonstrated experimentally (e.g. Payne *et al.* 1986) that the lifting vortices of a low-speed delta wing lie trapped above the swept leading edges and that the dorsal air flow reattaches to the wing medially. A number of models tackling this problem by modelling vortex sheets separating from the leading edge predict similar values of lift (reviewed by Parker 1976). The leading edge vortex (lev) model of Polhamus (1966, 1971; see also Hoerner 1975; Katz & Plotkin 1991) models lift by two components. The potential lift is the equivalent of the linear slender wing model, but is extended to larger α and to wings of different shapes by lifting surface methods, and vortex lift is estimated as the suction of linear leading edge vortices. The lift coefficient is

$$C_{L,lev} = k_p \sin\alpha\cos^2\alpha + k_v \sin^2\alpha\cos\alpha, \tag{5}$$

where k_p and k_v are the potential and vortex force constants, respectively, which for a thin, flat, triangular wing can be determined from the aspect ratio A by

$$k_p = 1.393A - 0.141A^2, \tag{6}$$

and

$$k_v = 3.157 - 0.020A + 0.021A^2, \tag{7}$$

for $0 \leqslant A \leqslant 4$ (digitized from figures in Polhamus (1966)). Vortex lift k_v varies only slightly with A. Different formulae for k_p apply for different planforms, such as sector, arrow or diamond shapes (Hoerner 1975), and it is no longer valid to ignore segments of a wing or tail behind the location of maximum continuous span. The leading edge vortex model predictions have been shown to be realistic for delta wings with A up to at least 3 and α up to 25° (Polhamus 1971; Parker 1976).

(d) *Lifting line model*

This is the conventional approximate model for a lifting wing in which the wingspan is much greater than the chord and lifting wake vortices are shed largely at the trailing edge. The lift coefficient can be estimated as

$$C_{L,LL} = \frac{mA}{(1+\tau)m/\pi + A}\alpha, \tag{8}$$

(Von Kármán & Burgers 1935), where m is a constant determined by the wing profile ($m = 2\pi$ for a thin, flat wing) and τ is determined by the wing planform shape and varies from zero for small A to 0.11 for $A = 4$ (computed by a method of Glauert (1947)). We are concerned here with tails with an aspect ratio A of less than 3, for which we do not consider the lifting line model appropriate. We include it here for comparison and because it could be more realistic than the leading edge vortex model for widely spread tails ($\theta > 50°$); in any case, the difference in predicted lift between the lifting line and leading edge vortex models for starling tails is small (figure 2).

4. RESULTS

Lift measured at 4.9 m s^{-1} on the starling body with a furled (0° spread) tail and $\alpha_b = 5°$ was 5.36 ± 1.39 mN at $\alpha = 5°$ and 11.99 mN at $\alpha = 15°$ (figure 1). These values are small (< 2%) compared to starling body weight (*ca.* 750 mN) and imply that the starling tail rarely makes a significant contribution to weight support in flight, but they are plausible compared to measured starling body and tail drag of 11–15 mN (Maybury 2000; Maybury & Rayner 2001). The slender wing model (§ 3b) predicts that lift is only determined by the maximum continuous tail span b_{max}, which when furled is 2.1 cm, giving a predicted tail lift of 0.9 mN at $\alpha = 5°$ and 2.7 mN at $\alpha = 15°$. If this model is realistic and if the components of lift generated by the tail and the body can be separated (see § 5c), then body lift at $\alpha_b = 5°$ and 4.9 m s^{-1} is between 5 and 10 mN or between one-third and one-half of body drag.

The total lift L_T on the starling body and tail and, therefore, also the incremental lift contributed by the tail L_t increases with tail spread θ (figure 1). All three theoretical models predict a significant increase in lift coefficient with tail spread ($r_{13} = 0.960$–0.997). In contradiction to these predictions, the measured tail lift coefficient C_{Lt} (0.383 ± 0.030) is independent of tail spread ($r_{13} = 0.093$ and $p = 76\%$) or aspect ratio (figure 2).

Lift predicted by the leading edge vortex and lifting line models is similar, differing most at the lowest tail spreads. The slender wing model predicts that C_{Lt} increases more steeply with tail spread, with markedly lower values (39% of the leading edge vortex model) when the tailed is furled, but higher values (128% of the leading edge vortex model) when spread. The potential component of the leading edge vortex model (figure 2) corrects the slender wing model for larger α and wider tail spreads. The two predictions are similar at lower spreads, but the slender wing model markedly overestimates the potential force at larger spreads and α because of its small disturbance linear assumptions. The

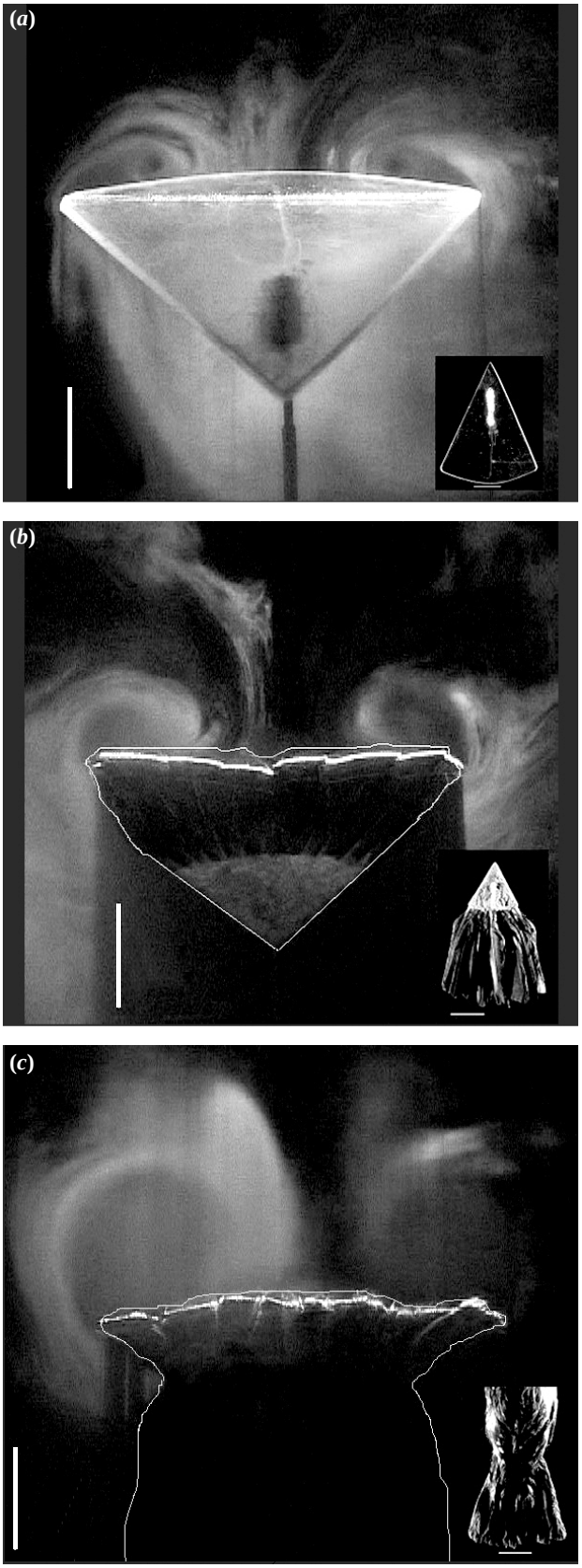

Figure 3. Visualization of leading edge vortices over model and real starling tails at air speed 4.9 m s^{-1}. In each case the tail apex angle is 50° ($\theta = 25°$) and $\alpha = 15°$. The tail is seen from upstream and at an oblique angle from above and is illuminated by a vertical laser sheet (Class 3A, 5-mW, 523-nm line-generating laser, Nu-Light Systems Ltd, Warrington, Cheshire WA5 1AH, UK) aligned with the maximum tail span, with air flow seeded by a JEM Technofogger smoke generator (Martin Professional plc, Maidstone, Kent ME15 9YG, UK). Insets show tail planform. Scale bars 20 mm (in visualization images correct for vertical axis). (*a*) Perspex model sector-shaped tail with well-developed spiral vortices close to the wing surface. (*b*) Isolated starling tail with the triangular apex region modelled in resin, also with clear leading edge vortices. At this relatively modest tail spread the tail rectrices are extensively overlapped and the tail has a sector planform. Compared with (*a*) the vortex centres are significantly ($F_{1,18} = 212$) nearer the tail tips, hypothetically because the leading edge is not straight owing to feather curvature or because the tail is not flat or because the feathered tail deforms elastically. (*c*) A complete starling body and tail (body angle of attack $\alpha_b = 5°$, as for force measurements in figures 1 and 2). The configuration of the distal tail rectrices is as in (*b*). Leading edge vortices are still present, but are more diffuse and their spiral structure is less evident and they lie higher above the tail surface and, therefore, contribute less to tail lift. Ten images of each tail were taken with a Sony DC 3CCD digital camcorder digitized with DVRaptor video version 1.13 (Canopus Corporation, San José, CA, USA), enhanced and measured with Scion Image, version beta 2 (Scion Corporation, Frederick, MD, USA).

vortex lift component of the leading edge vortex model varies little with tail spread (equation (7) and § 3c).

The measured lift coefficient is in the range of the predictions of all three models at the lowest tail spreads, i.e. up to *ca*. $\theta = 5°$, but at higher spreads falls significantly below all of the predictions (figure 2). The potential component of the leading edge vortex model alone is a substantial overestimate for tail spreads greater than 15° and the leading edge vortex model including the vortex suction forces overestimates the measured increment in lift by factors of up to 2.3. The slender wing model underestimates the measured lift coefficient by 73% when the tail is furled, but at larger spreads increasingly overestimates lift (by a factor of 2.95 at a tail spread of 32°).

5. DISCUSSION

(a) *Bird tail aerodynamics and delta wing models*

Our aim was to test how well theoretical models of delta wing aerodynamics predict measured lift on the starling tail. None of the available model predictions was adequate; all models overestimate tail lift at moderate but typical tail spreads and angle of attack and fail to capture the measured uniformity in the lift coefficient with tail spread. We know of no theoretical model that predicts this result and, accordingly, have no prediction as to how the lift coefficient might depend on the angle of attack (of the body or of the tail) or on air speed. The leading edge vortex model comes closest to predicting the air flow over the tail (figures 3 and 4), but there remain important differences and this model overestimates tail lift.

Thomas (1993) asserted that the slender wing model should apply to bird tails, but our results show this to be the least accurate of the available models. For several reasons, we do not recommend the use of this model. First, it is not realistic: an increase in tail aspect ratio does not increase the measured lift coefficient. Second, small changes in tail shape have a greater effect on lift and on air flow over the tail than would be expected from this model (figure 4). Third, when the model has been used to predict optimum tail size and shape (Balmford

et al. 1993; Thomas 1993; Thomas & Balmford 1995), the optimal tail lift/drag ratio was expected to occur with tails spread at 60° (120° apex angle), but this degree of spread lies well beyond the range for which slender wing theory can be valid for an isolated delta wing, even at low α. The model has been used to quantify the balance between, on the one hand, natural selection on optimal tail size for aerodynamic performance and, on the other, enlarged tail size in response to sexual selection (e.g. Thomas & Balmford 1995; Møller *et al.* 1998; Barbosa & Møller 1999). The slender wing hypothesis overemphasizes the aerodynamic advantage of a tail of given length or spread and, accordingly, underestimates the aerodynamic optimal tail feather length. The failure of this model therefore has consequences for the ongoing debate surrounding selective pressures on the morphology of ornamented tails. Notwithstanding the problems with the slender wing model, comparative tests (Balmford *et al.* 1993; Balmford & Thomas 1995) appear to support qualitative predictions. Furthermore, Buchanan & Evans (2000) and Park *et al.* (2000) have demonstrated in recent empirical studies of flight performance in hirundines that, as previously argued theoretically (Evans & Thomas 1997), forked tails are longer than the aerodynamic optimum for certain measures of flight performance. There is no reason from our results to question the importance of sexual selection in the evolution of ornamented feathers in barn swallow tails.

(b) *Body–tail interactions*

Our force measurements and flow visualizations show that it is not possible to derive a simple prediction of lift or drag for the avian tail based on tail morphology, and that the body and tail cannot be considered in isolation of each other. We have not attempted to determine starling tail drag by similar methods to those we used for lift because we have determined elsewhere (Maybury & Rayner 2001) that drag is dominated by interactions between the body and tail. A comparable incremental model would predict that tail drag is roughly proportional to tail area. Thomas (1993) used a laminar boundary layer (on one side of the tail) to estimate tail profile drag from tail length and span. However, progressive shortening and removal of the starling tail significantly increases the drag of the combined body and tail by altering how air flows over the dorsal body surface and how the ventral boundary layer separates and reattaches (Maybury & Rayner 2001); a key part of this mechanism in starlings appears to be that the posterior dorsal boundary layer is turbulent. Total body and tail drag cannot be determined from tail size (contra Thomas 1993) and control of total drag may be of comparable importance to tail lift in determining the effect on tail morphology of natural selection for aerodynamic performance.

The aerodynamics of the avian tail are critically determined by body–tail interactions. On a sector-planform model or an isolated starling tail, vortices are, as expected for a delta wing, trapped over the leading edge (figures 3*a*,*b* and 4*a*,*b*) and measured tail lift conforms reasonably well to predictions of Polhamus' (1966, 1971) leading edge vortex theory (Maybury 2000; W. J. Maybury, M. R. Evans and J. M. V. Rayner, unpublished results). On the intact starling (figures 3*c* and 4*c*), with its streamlined, slender lifting body anterior to the spread tail, both lift force and the vortex flow over the tail differ substantially: the vortices are larger and more diffuse, their centres are located significantly higher above the tail trailing edge than for the isolated tail (13.8 ± 1.7 mm

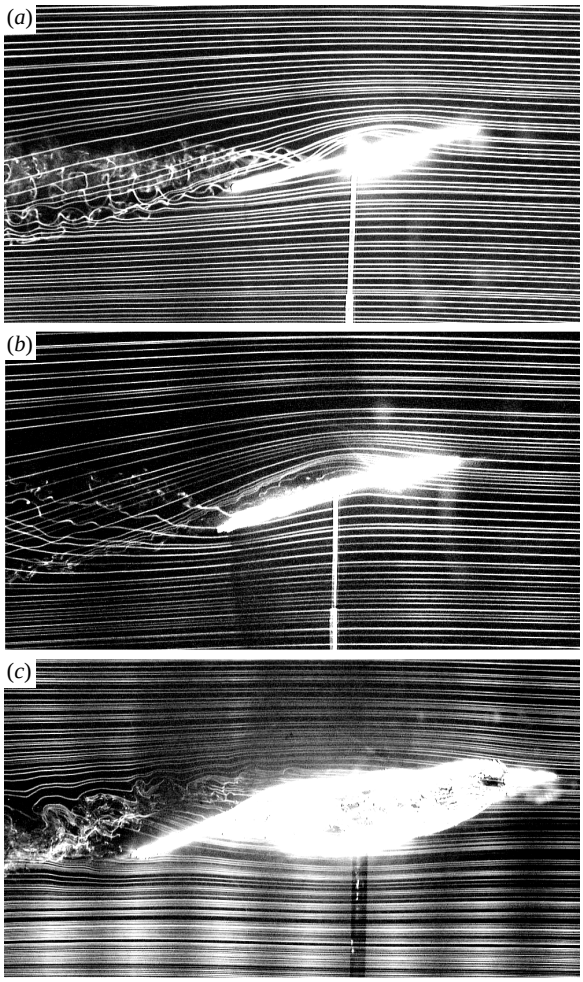

Figure 4. Side views of flow development of vortices and wake, with geometry as in figure 3, visualized by the oil wire method (Maybury & Rayner 2001). Tail apex angle $\theta = 25°$, angle of attack $\alpha = 15°$ and air speed = 4.9 m s^{-1}). (*a*) A sector planform Perspex wing. (*b*) Isolated starling tail. (*c*) Intact starling body and tail. In (*a*) and (*b*) the vertical plane of smoke streamers meets the tail *ca.* 25% along the leading edge, whereas in (*c*) the streamers graze the broadest part of the body and meet the tail at *ca.* 75% along the leading edge. A clear leading edge vortex develops over the model sector wing and flow reattaches medially and the vortices remain distinct but become turbulent above the trailing edge. Flow is similar over the isolated starling tail, but the vortex is broader in dimension and appears to remain laminar. Flow is radically different over the intact bird; the tail still generates lift, as is evidenced by the upward suction of streamlines below the ventral covert feathers, but the turbulent trailing vortices that generate this suction appear anteriorally over the body and lie higher above the tail (cf. figure 3); no further vortices develop either on or above the tail. Images are illuminated with four synchronized Metz flash guns (one-sixteenth power) and are captured by a Nikon E3s Digital Camera (effective ISO800, shutter speed 0.125 s, 35–70 mm f2.8 AF-D Nikkor lens at aperture f8) and enhanced in Paint Shop Pro v. 5. Both camera and smoke wire were triggered manually.

compared to 8.7 ± 0.7 mm) ($F_{1,18} = 77.8$), and vortices above the tail originate forward over the body (figure 4*c*). This increase in the distance between the vortices and the tail surface reduces the area for medial flow reattachment and thereby reduces the suction force on the dorsal side of the tail; this explains why the incremental tail lift measured here is lower than expected from an isolated tail (figure 2).

The development of lifting leading edge vortices on a delta wing depends critically on the shape of the apex and the air flow around it. At moderate tail spread the tail is comparable in width to the body and, therefore, operates within the body wake. At small incidence α_b the body is generating lift and it must therefore generate a system of trailing vortices, which for a slender body at incidence separate near the apex and then follow the body contour (e.g. Hoerner 1975). On a starling body these vortices develop as a 'scarf vortex' formed at the laminar separation bubble behind the neck (Maybury & Rayner 2001). We hypothesize that the mechanism of body–tail lift interaction in birds is that downstream these vortices lie above the tail where they absorb vortex sheets shed from the leading edges of the tail (figure 4*c*). Thus, the tail generates some lift, but not as much as if it was an isolated delta wing.

Our examples of significant body–tail interactions in determining both lift and drag reveal that it is unrealistic to consider the force-generating elements of the body in isolation. Here we have considered the body and tail independently of the wings. We expect that, in free-flying birds, interactions between the tail and trailing vortices from the wings (as considered for rigid wings by Hummel (1992) and Thomas (1996)) and the effect of the flapping wings on the body boundary layer will have significant effects on tail aerodynamics. Future experiments will explore these mechanisms with the aims of identifying whether the tail lift coefficient is generally independent of tail spread, and of deriving methods for estimating tail lift and drag from body and tail morphology so that selection for optimal tail morphology can be reassessed on a sound aerodynamic basis.

These experiments were funded by Biotechnology and Biological Sciences Research Council research grant S03843 to J.M.V.R. W.J.M. was supported by a research studentship from the Biotechnology and Biological Sciences Research Council and L.B.C. by the Universities of Bristol and Leeds. The wind tunnel fan was provided by the London Fan Company. We thank Sally Ward for video films of starlings in flight, Arthur Goldsmith for supplying the starling specimens, Paolo Viscardi for video digitizing and Matthew Evans for collaboration in some preliminary model delta wing experiments.

6. REFERENCES

Balmford, A., Thomas, A. L. R. & Jones, I. L. 1993 Aerodynamics and the evolution of long tails in birds. *Nature* **361**, 628–631.

Barbosa, A. & Møller, A. P. 1999 Aerodynamic costs of long tails in male barn swallows *Hirundo rustica* and the evolution of sexual size dimorphism. *Behav. Ecol.* **10**, 128–135.

Bonser, R. H. C. & Rayner, J. M. V. 1996 Measuring leg thrust forces in the common starling. *J. Exp. Biol.* **199**, 435–439.

Buchanan, K. L. & Evans, M. R. 2000 The effect of tail streamer length on aerodynamic performance in the barn swallow. *Behav. Ecol.* **11**, 228–238.

Evans, M. R. & Thomas, A. L. R. 1997 Testing the functional significance of tail streamers. *Proc. R. Soc. Lond.* B **264**, 211–217.

Glauert, H. 1947 *The elements of aerofoil and airscrew theory.* Cambridge University Press.

Hoerner, S. F. 1975 *Fluid dynamic lift: practical information on aerodynamic and hydrodynamic lift.* Brick Town, NJ: L. A. Hoerner.

Hummel, D. 1992 Aerodynamic investigations on tail effects in birds. *Z. Flugwiss. Weltraumforsch.* **16**, 159–168.

Jones, R. T. 1946 Properties of low-aspect-ratio pointed wings at speeds below and above the speed of sound. *NACA Rep.* **835**.

Jones, R. T. 1990 *Wing theory.* Princeton University Press.

Katz, J. & Plotkin, A. 1991 *Low-speed aerodynamics: from wing theory to panel methods.* New York: McGraw-Hill.

Maybury, W. J. 2000 The aerodynamics of bird bodies. PhD thesis, University of Bristol, Bristol, UK.

Maybury, W. J. & Rayner, J. M. V. 2001 The avian tail reduces body parasite drag by controlling flow separation and vortex shedding. *Proc. R. Soc. Lond.* B **268**, 1405–1410.

Møller, A. P. 1994 *Sexual selection and the barn swallow.* Oxford University Press.

Møller, A. P., De Lope, F. & Saino, N. 1995 Sexual selection in the barn swallow *Hirundo rustica*. 6. Aerodynamic adaptations. *J. Evol. Biol.* **8**, 671–687.

Møller, A. P., Barbosa, A., Cuervo, J. J., De Lope, F., Merino, S. & Saino, N. 1998 Sexual selection and tail streamers in the barn swallow. *Proc. R. Soc. Lond.* B **265**, 409–414.

Norberg, U. M. 1990 *Vertebrate flight.* Heidelberg: Springer.

Norberg, R. Å. 1994 Swallow tail streamer is a mechanical device for self-deflection of tail leading edge, enhancing aerodynamic efficiency and flight manoeuvrability. *Proc. R. Soc. Lond.* B **257**, 227–233.

Park, K. J., Evans, R. M. & Buchanan, K. L. 2000 Assessing the aerodynamic effects of tail elongations in the house martin (*Delichon urbica*): implications for the initial selection pressures in hirundines. *Behav. Ecol. Sociobiol.* **48**, 364–372.

Parker, A. G. 1976 Aerodynamic characteristics of slender wings with sharp leading edges–a review. *J. Aircraft* **13**, 161–168.

Payne, F. M., Ng, T. T., Nelson, R. C. & Schiff, L. B. 1986 Visualization and wake surveys of vortical flow over a delta wing. *AIAA J.* **26**, 137–143.

Pennycuick, C. J. 1975 Mechanics of flight. In *Avian biology*, vol. V (ed. D. S. Farner, J. R. King & K. C. Parkes), pp. 1–73. New York: Academic Press.

Pennycuick, C. J., Obrecht, H. H. & Fuller, M. R. 1988 Empirical estimates of body drag in large waterfowl and raptors. *J. Exp. Biol.* **135**, 253–264.

Polhamus, E. C. 1966 A concept of the vortex lift of sharp-edge delta wings based on a leading-edge suction analogy. *NASA TN* D–**3767**.

Polhamus, E. C. 1971 Predictions of vortex-lift characteristics by a leading-edge suction analogy. *J. Aircraft* **8**, 193–199.

Rae, W. H. & Pope, A. 1984 *Low-speed wind tunnel testing*, 2nd edn. New York: Wiley-Interscience.

Rayner, J. M. V., Viscardi, P. W., Ward, S. & Speakman, J. R. 2001 Aerodynamics and energetics of intermittent flight in birds. *Am. Zool.* (In the press.)

Thomas, A. L. R. 1993 On the aerodynamics of birds' tails. *Phil. Trans. R. Soc. Lond.* B **340**, 361–380.

Thomas, A. L. R. 1996 Why do birds have tails? The tail as a drag reducing flap and trim control. *J. Theor. Biol.* **183**, 247–253.

Thomas, A. L. R. & Balmford, A. 1995 How natural selection shapes birds' tails. *Am. Nat.* **146**, 848–868.

von Kármán, T. & Burgers, J. M. 1935 General aerodynamic theory—perfect fluids. In *Aerodynamic theory*, vol. II (ed. W. F. Durand), pp. 1–367. Berlin: Springer.

Ward, S., Rayner, J. M. V., Möller, U., Jackson, D. M., Nachtigall, W. & Speakman, J. R. 1999 Heat transfer from starlings *Sturnus vulgaris* during flight. *J. Exp. Biol.* **202**, 1589–1602.